Event-triggered Asynchronous Distributed MPC for Multi-Quadrotor Systems with Communication Delays

Chun Liu[1], Yupeng Shu[1], Liang Xu[1], Yihuan Jin[2], Guijia Xu[2], Kuan Li[2], and Hongtian Chen[3]

[1]Shanghai University
[2]SAST Shanghai Spaceflight Precision Machinery Institute
[3]Shanghai Jiao Tong University

June 21, 2024

Abstract

This paper investigates the formation composition and keeping problem for multi-quadrotor systems under time-varying communication delays. First, a distributed model predictive control (MPC) approach is employed to transform the formation composition and keeping of multi-quadrotor systems into an online rolling optimization issue, accompanied by the event-triggered mechanism to reduce solution frequency and communication load. Second, to address the asynchrony and time-varying communication delays introduced by event-triggered distributed MPC, a set of constraints is designed to restrict deviations between the current predictive state and previously broadcasted states. Consequently, based on the previously predicted states of neighbors, the cooperation of the multi-quadrotor systems is achieved under asynchronous communication and time-varying delays. This approach guarantees robust asymptotic stability and satisfactory formation performance for multi-quadrotor systems under various delay scenarios. Finally, the numerical and software-in-the-loop (SIL) simulations validate the effectiveness of the proposed algorithm of multi-quadrotors under communication delays.

figures/figure-1/figure-1-eps-converted-to.pdf

figures/figure-2/figure-2-eps-converted-to.pdf

figures/figure-3a/figure-3a-eps-converted-to.pdf

figures/figure-3b/figure-3b-eps-converted-to.pdf

figures/figure-4a/figure-4a-eps-converted-to.pdf

figures/figure-4b/figure-4b-eps-converted-to.pdf

figures/figure-5a-phi/figure-5a-phi-eps-converted-to.pdf

figures/figure-5a-psi/figure-5a-psi-eps-converted-to.pdf

figures/figure-5a-theta/figure-5a-theta-eps-converted-to.pdf

figures/figure-5a-x/figure-5a-x-eps-converted-to.pdf

figures/figure-5a-y/figure-5a-y-eps-converted-to.pdf

figures/figure-5a-z/figure-5a-z-eps-converted-to.pdf

figures/figure-5b-phi/figure-5b-phi-eps-converted-to.pdf

figures/figure-5b-psi/figure-5b-psi-eps-converted-to.pdf

figures/figure-5b-theta/figure-5b-theta-eps-converted-to.pdf

figures/figure-5b-x/figure-5b-x-eps-converted-to.pdf

figures/figure-5b-y/figure-5b-y-eps-converted-to.pdf

figures/figure-5b-z/figure-5b-z-eps-converted-to.pdf

figures/figure-6a/figure-6a-eps-converted-to.pdf

figures/figure-6b/figure-6b-eps-converted-to.pdf

figures/figure-7a/figure-7a-eps-converted-to.pdf
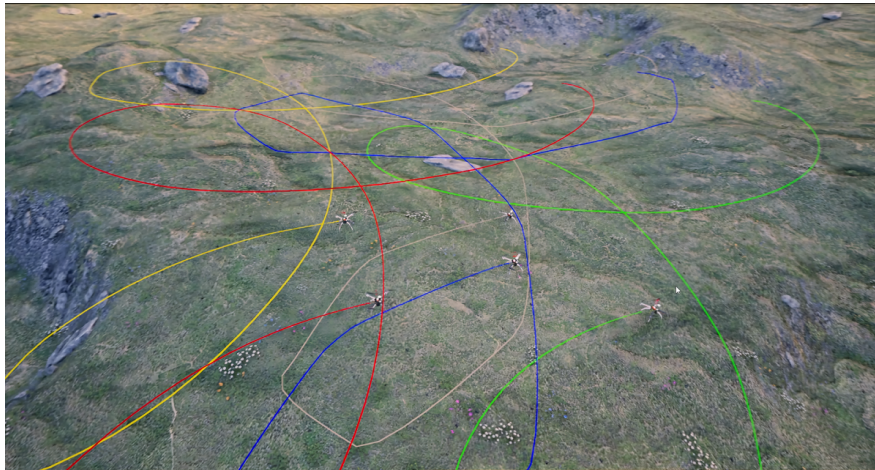
Event-triggered Asynchronous Distributed MPC for Multi-Quadrotor Systems with Communication Delays

Yupeng Shu[1] | Chun Liu*[1,2] | Liang Xu[2] | Yihuan Jin[3,4] | Guijia Xu[3] | Kuan Li[3,5] | Hongtian Chen[6]

[1]School of Mechatronic Engineering and Automation, Shanghai University, Shanghai, China

[2]School of Future Technology (Institute of Artificial Intelligence), Shanghai University, Shanghai, China

[3]Shanghai Aerospace Control Technology Institute, Shanghai, China

[4]Control Technology Research and Development Center of the Eighth Academy, Shanghai, China

[5]Shanghai Engineering Research Center of Servo Systems, Shanghai, China

[6]Department of Automation, Shanghai Jiao Tong University, Shanghai, China

Correspondence
Chun Liu, School of Mechatronic Engineering and Automation, Shanghai University, Shanghai 200444, China
E-mail: Chun_Liu@shu.edu.cn

Abstract

This paper investigates the formation composition and keeping problem for multi-quadrotor systems under time-varying communication delays. First, a distributed model predictive control (MPC) approach is employed to transform the formation composition and keeping of multi-quadrotor systems into an online rolling optimization issue, accompanied by the event-triggered mechanism to reduce solution frequency and communication load. Second, to address the asynchrony and time-varying communication delays introduced by event-triggered distributed MPC, a set of constraints is designed to restrict deviations between the current predictive state and previously broadcasted states. Consequently, based on the previously predicted states of neighbors, the cooperation of the multi-quadrotor systems is achieved under asynchronous communication and time-varying delays. This approach guarantees robust asymptotic stability and satisfactory formation performance for multi-quadrotor systems under various delay scenarios. Finally, the numerical and software-in-the-loop (SIL) simulations validate the effectiveness of the proposed algorithm of multi-quadrotors under communication delays.

KEYWORDS:
Multi-quadrotor systems, distributed MPC, event-triggered mechanism, formation composition and keeping, communication delays

1 | INTRODUCTION

Collaborative execution of diverse tasks by multi-quadrotor systems stands as a crucial trend in the application of unmanned aerial vehicle systems, encompassing activities such as area reconnaissance, logistics delivery, synergy mapping, search and rescue, etc.[1-5] The latest advancements in the collaborative control of multiple unmanned aerial vehicle systems have been comprehensively reviewed.[6] Formation control, particularly the composition and keeping of formation, constitutes a core element in the collaborative operation of multi-quadrotor systems.[7] However, during the execution of practical tasks, multi-quadrotor

systems are susceptible to various physical and networked constraints, including state constraints, control saturation constraints, communication delays, and packet loss.[8–10]

From the perspective of formation control, employing distributed control with local information is especially suitable for multi-quadrotor systems with numerous autonomous nodes. However, the network communication characteristics of multi-quadrotor systems based on distributed control strategies can lead to the following two key issues. 1) High-intensity communication loads lead to a decrease in the precision performance of multi-quadrotor formation control. 2) Limited communication bandwidth may result in phenomena such as communication delays and packet loss in multi-quadrotor systems. In addressing the first problem, the distributed model predictive control (DMPC) strategy is considered to possess advantages compared to existing control methods such as the linear quadratic regulator,[11] sliding mode control,[12] active disturbance rejection control,[13] etc. DMPC is recognized for its capability in handling constraints and enhancing system flexibility. It is regarded as an effective approach for addressing both the physical and networked constraints in multi-quadcopter systems. For example, a DMPC method based on the chaotic grey wolf optimization algorithm is proposed for coordinating the control of multiple unmanned aerial vehicle systems.[14] In practical applications, there are also solutions based on DMPC to address the collaborative payload transport challenges in multi-quadrotor systems.[15] For the communication problem, the utilization of a periodic DMPC strategy in practical multi-quadrotors, where computational and network resources are typically limited, will result in unnecessary computation and communication overhead. Therefore, the widespread adoption of event-triggered schemes, which transmit data based on predefined triggering conditions, serves as an effective approach to reduce computational and communication costs.[16–18] In addition, the proposed event-triggered mechanism (ETM) framework encompasses various strategies, namely, a statistical learning-based ETM,[19] a delay compensation-based ETM,[20] and a dual-mode-based ETM.[21] This framework aims to ensure control performance by minimizing the occurrence of event triggers. This reduction is crucial for conserving network resources and maintaining both recursive feasibility and stability through the inclusion of robustness constraints. Therefore, to address the aforementioned challenges, the introduction of event-triggered distributed model predictive control (EDMPC) as a necessary but challenging approach for the formation and keeping of multi-quadrotor systems is essential.

The formation and keeping control of multi-quadrotor systems with integrated distributed ETM faces challenges posed by asynchronous communication networks. The asynchronous nature arises from the different triggering events and communicating instants of various quadrotors, resulting in reduced real-time performance and stability of the overall system.[22] It is noteworthy that communication delays, as typical networked elements, exhibit more pronounced characteristics in asynchronous systems, thereby posing a significant threat to the stability of multi-quadrotor systems. In response to communication latency issues, initial efforts have employed MPC methods to achieve formation flight control for multi-quadrotor systems with communication delays.[23] Additionally, a second-order multi-agent formation control method based on neighbor information feedback control is proposed to mitigate the impact of communication delays between different agents.[24] However, these studies do not delve deeply into the asynchronous communication issues and system stability problems caused by delays. To mitigate communication latency issues in asynchronous systems, approaches such as self-triggered DMPC methods or the utilization of neural networks for compressing data packets have been adopted.[25–27] Despite these methods considering the effects of asynchronous communication, they do not explicitly address the estimation error problem arising from asynchronous communication.

To address the aforementioned challenges and effectively manage state and input constraints in multi-quadrotor systems, this paper introduces an EDMPC method. This strategy overcomes the limitations of traditional MPC, such as high computational load and frequent communication requirements, while maintaining the advantages of handling system constraints, reducing communication burden, and optimizing control performance. The key innovations and summarizations in this paper are outlined as follows.

(1) A novel class of EDMPC strategy is implemented to mitigate the bandwidth usage in the communication topology of multi-quadrotor systems while achieving high-precision formation and maintenance. Consideration is given to the limited computational capacity of onboard devices and the reduced communication frequency within multi-quadrotor systems, providing support for the stable formation composition and keeping control of multi-quadrotor systems.

(2) Addressing the challenge of bounded time-varying communication delays in real-time information exchange among multi-quadrotor systems, a conceptual framework is proposed. This framework integrates predicted state information with compensatory state information and combines them into a comprehensive information set transmitted to neighboring quadrotors. Furthermore, a set of constraints on the transmitted states is designed to limit the deviation between the previously broadcasted state and the current predicted state. This ensures the stability of the formation configuration of the multi-quadrotor systems in the presence of communication delays while reducing the risk of individual quadrotors in the cluster losing connection or colliding.
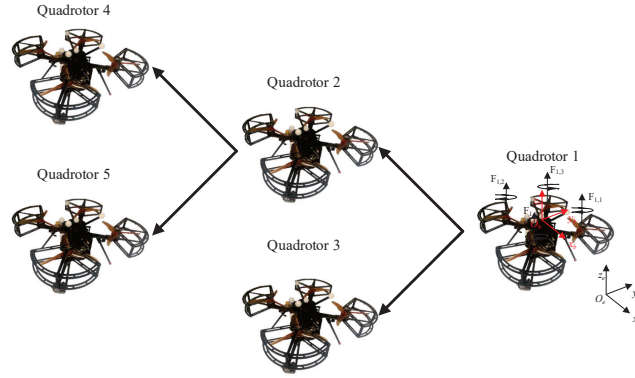
FIGURE 1 Directed graph $\mathcal{G}$ of multi-quadrotor systems and schematic diagram of the quadrotor.

The remainder of this paper is formulated as follows. Section 2 presents the modeling of the quadrotor system and control objectives. Section 3 introduces the time-triggered mechanism and optimization problems. Theoretical analysis of recursive feasibility and closed-loop stability are provided in Section 4. Section 5 conducts numerical simulations and SIL studies. Finally, Section 6 presents the conclusions.

2 | PRELIMINARIES AND CONTROL OBJECTIVE

2.1 | Quadrotor modeling

Consider multi-quadrotor systems composed of N quadrotors. The communication topology among quadrotors is described by a directed graph $\mathcal{G}(\mathcal{M}, \mathcal{L})$ with $\mathcal{L} := \{(i, j) | i, j \in \mathcal{M}, i \neq j\}$ and $\mathcal{M} := \{1, 2, ..., N\}$. Let $\mathcal{N}_i = \{j \mid (i, j) \in \mathcal{L}\}$ denotes the set of indices representing the neighbors of quadrotor i. An edge $(i, j) \in \mathcal{L}$ means that quadrotor i can send a message to quadrotor j. To elucidate the dynamics of a singular quadrotor, [28] it is imperative to define two distinct coordinate systems: the geodetic coordinate system, denoted as $E(X_e, Y_e, Z_e)$, and the fuselage coordinate system, denoted as $B(X_b, Y_b, Z_b)$. As illustrated in Figure 1, the dynamics of the i-th quadrotor ($i = 1, 2, ..., N$) can be formally articulated in the following manner:

$$
\begin{cases}
\ddot{x}_i = -\frac{U_{i,4}}{m}(\cos \psi_i \sin \theta_i \cos \phi_i + \sin \psi_i \sin \phi_i) \\
\ddot{y}_i = -\frac{U_{i,4}}{m}(\sin \psi_i \sin \theta_i \cos \phi_i - \cos \psi_i \sin \phi_i) \\
\ddot{z}_i = g - \frac{U_{i,4}}{m} \cos \phi_i \cos \theta_i \\
\ddot{\phi}_i = \frac{1}{I_{xx}}(U_{i,1} + q_i r_i (I_{yy} - I_{zz})) \\
\ddot{\theta}_i = \frac{1}{I_{yy}}(U_{i,2} + p_i r_i (I_{zz} - I_{xx})) \\
\ddot{\psi}_i = \frac{1}{I_{zz}}(U_{i,3} + p_i q_i (I_{xx} - I_{yy}))
\end{cases}
\tag{1}
$$

where (x_i, y_i, z_i) represent the positional coordinates of the i-th quadrotor, $(\theta_i, \phi_i, \psi_i)$ represent the pitch, roll, and yaw angles of the i-th quadrotor, respectively. Moreover, the term (p_i, q_i, r_i) represents the angular velocities of the i-th quadrotor in the body coordinate system. The parameter m represents the mass of the i-th quadrotor, while g denotes the gravitational acceleration. The input variables $U_{i,1}$, $U_{i,2}$, and $U_{i,3}$ are the driving torques in the roll, pitch, and yaw direction, respectively. Additionally, $U_{i,4}$ demonstrates a linear relationship with the lift force. The rotational inertia about the x, y, and z axes in the body coordinate system is denoted by I_{xx}, I_{yy}, and I_{zz}, respectively. The horizontal and vertical movement of quadrotor i is achieved by the thrust and torque generated from the rotation of the propellers. The torque vector that drives the quadrotor is defined as follows:

$$
\begin{bmatrix}
U_{i,1} \\
U_{i,2} \\
U_{i,3} \\
U_{i,4}
\end{bmatrix}
=
\begin{bmatrix}
-d F_{i,1} + d F_{i,2} + d F_{i,3} - d F_{i,4} \\
-d F_{i,1} - d F_{i,2} + d F_{i,3} + d F_{i,4} \\
-M_{i,1} + M_{i,2} + M_{i,3} - M_{i,4} \\
F_{i,1} + F_{i,2} + F_{i,3} + F_{i,4}
\end{bmatrix}
\tag{2}
$$

where $F_{i,1}, ..., F_{i,4}$ and $M_{i,1}, ..., M_{i,4}$ represent the thrust and counter-rotating torque of the propellers, respectively. d represents the arm length of the quadrotor. The values of $F_{i,n}$ and $M_{i,n}$ can be approximately expressed as:

$$\begin{cases} F_{i,n} = c_t \Omega_n^2, & n = 1, 2, 3, 4 \\ M_{i,n} = c_\tau \Omega_n^2, & n = 1, 2, 3, 4 \end{cases} \tag{3}$$

where Ω_n represents the rotational speed of the n-th motor, c_t and c_τ denote the thrust coefficient and the drag coefficient, respectively.

Assumption 1: The permissible angles for maneuvering are notably constrained to values significantly smaller than those conducive to gimbal locking under practical conditions during quadrotor attitude control. Consequently, the attitude control system is consistently upheld with minor perturbations. Hence, the quadrotor flight can be effectively approximated under conditions of small perturbations, governed by the following relationships: $\dot{\phi}_i = p_i$, $\dot{\theta}_i = q_i$, and $\dot{\psi}_i = r_i$.

An EMPC algorithm is proposed for the quadrotor system.[29] The algorithm is integrated into multi-quadrotor systems, with each rotor controlled to follow its corresponding reference quadrotor. The position of the reference quadrotor is determined by combining the position information of the leader quadrotor with a predefined formation. The state vector and input vector are defined as $\xi_i = [x_i \, \dot{x}_i \, y_i \, \dot{y}_i \, z_i \, \dot{z}_i \, \phi_i \, \dot{\phi}_i \, \theta_i \, \dot{\theta}_i \, \psi_i \, \dot{\psi}_i]^T$ and $u_i = [U_{i,1} \, U_{i,2} \, U_{i,3} \, U_{i,4}]^T$, respectively. The quadrotor system can be expressed by the following system:

$$\dot{\xi}_i(t) = f_i(\xi_i(t), u_i(t)) + \omega_i(t) = f_i(\xi_i(t), u_i(t), \omega_i(t)) \tag{4}$$

where $\omega_i(t)$ represents the additive disturbance experienced by the i-th quadrotor system.

Assumption 2: Within the individual channels corresponding to distinct facets of flight control, encompassing considerations for external perturbations such as the influence of airflow on flight speed or uncertainties in the intrinsic characteristics of the quadrotor, all such effects are constrained within predefined known upper limits. This constraint is mathematically articulated through the conditions $||\omega_i(t)|| \leq \overline{\omega}$.

Assumption 3: There exist constants $L_p, \nu \in \mathbb{R}_{\geq 0}$ such that the conditions $||f(\xi, u) - f(\iota, u)|| \leq L_p ||\xi - \iota||$ and $||f(x, u, \omega) - f(x, u, \omega_0)|| \leq \nu ||\omega - \omega_0||$ hold for all $\xi, \iota \in \Omega$, $u \in \mathcal{U}$, $i \in \mathcal{M}$.

Assumption 4: For quadrotor i, the local sampling instant t_k^i and the communication delays τ_k^{ij}, satisfy: $1 \leq t_{k+1}^i - t_k^i \leq \bar{H}$ and $0 < \tau_k^{ij} \leq \bar{\tau}$. The largest admissible sampling interval $\bar{H}$ and the largest communication delay $\bar{\tau}$ are constrained within predefined known upper limits. There is no disordering transmission among quadrotors.

2.2 | Control objective

The control objective is to design a novel EDMPC strategy for the formation and keeping of multi-quadrotor systems, considering parameter uncertainties and external disturbances. The strategy aims to achieve the following two goals without the need for high-frequency optimization solutions and intense information exchange, despite the presence of external disturbances, communication delays, and input constraints.

R1) Formation and keeping of the multi-quadrotor systems according to a predetermined formation is achieved to accomplish the assigned task, with the formation error below a specified threshold.

R2) It is guaranteed that the EDMPC scheme in the multi-quadrotor systems is recursively feasible and stable.

3 | EDMPC FOR MULTI-QUADROTOR SYSTEMS WITH COMMUNICATION DELAYS

This section introduces an EDMPC framework designed for multi-quadrotor systems. The primary goal is to guide the formation error of the entire multi-quadrotor systems toward predefined regions proximate to the origin while concurrently ensuring system stability. In Section 3.1, the exploration of time-varying communication delays among multi-quadrotor systems is explained, providing an impartial analysis of this phenomenon. Section 3.2 delves into the formulation of the optimization problem intrinsic to MPC. Subsequently, an ETM is outlined to describe the procedure for identifying optimal time instances for solving the relevant optimization problem.

3.1 | Asynchronous communication with time-varying delays

Define the sequence t_k^i as the optimization time, quadrotor i broadcasts the latest predicted position state sequence to its neighbors, which is constructed as:

$$\xi_i^b(s|t_k^i) = \begin{cases} \xi_i^*(s|t_k^i), & s \in [t_k^i, t_k^i + T) \\ \xi_i^*(t_k^i + T|t_k^i), & s \in [t_k^i + T, t_{k+1}^i + \bar{\tau}] \end{cases} \tag{5}$$

where $\xi_i^*(s|t_k^i)$ denotes the optimal predicted position state, and $\xi_i^*(t_k^i + T|t_k^i)$ denotes the final optimal predicted state. The relationship between the triggering interval and the triggering time is given by $t_{k+1}^i = t_k^i + H^i(t_k^i)$.

In asynchronous multi-quadrotor systems, the concept of bounded time-varying communication delays is illustrated. Here, $\xi_j^b(t_k^{ij})$ represents the latest message broadcasted by quadrotor j, where $j \in \mathcal{N}_i$ at the timestamp t_k^{ij}. The temporal reference t_k^{ij} is formally defined as $t_k^{ij} = \max\{t_l^j \in I \mid t_l^j < t_k^i\}$. The communication delays can be classified into two distinct types:

CASE 1 : $t_k^i - t_k^{ij} < \tau_k^{ij} \leq \bar{\tau}$. This case indicates that quadrotor i, when solving the optimization problem at time t_k^i, does not receive the latest state message from quadrotor j. Therefore, it is necessary to use the historical state message from quadrotor j.

CASE 2 : $0 \leq \tau_k^{ij} \leq t_k^i - t_k^{ij}$. This case represents quadrotor i, when solving the optimization problem at time t_k^i, has already received the latest state message from quadrotor j.

Therefore, when constructing the local optimization problem for quadrotor i, based on the communication topology graph $\mathcal{G}$, the predicted state message $\xi_j^b(t_k^j)$ is obtained from its neighboring quadrotor j. Utilizing the preloaded desired formation information e_r^{ij}, where $\|e_{ij}\| < \alpha$, the solution for its own desired state trajectory is obtained through the following process:

$$\xi_{i,r}(t_k^{ij}) = \left(\xi_j^b(t_k^i|t_k^i) + e_r^{ij}, \cdots, \xi_j^b(t_k^i + T|t_k^i) + e_r^{ij} \right) \tag{6}$$

Therefore, the objective function for formulating the EDMPC optimization problem is provided as follows:

$$J_i(t_k^i) = \int_{t_k^i}^{t_k^i + T} L_i(s|t_k^i) ds + g_i(t_k^i + T|t_k^i)$$

where $J_i(t_k^i) = J_i(\xi_i(t_k^i), \xi_{i,r}(t_k^i), u_i(t_k^i))$, $L_i(t_k^i) = L_i(\xi_i(t_k^i), \xi_{i,r}(t_k^i), u_i(t_k^i))$, $g(t_k^i + T|t_k^i) = g(\xi_i(t_k^i + T|t_k^i))$, with the system sampling time Δt, the prediction horizon N, and $T = N \cdot \Delta t$ representing the prediction time. $H^i(t_i^k)$ denotes the time interval between two optimizations for quadrotor i. The term $\xi_i(t_k^i) = \left(\xi_i(t_k^i|t_k^i), \ldots, \xi_i(t_k^i + T|t_k^i) \right)$ denotes the collection of the predicted state sequence, and $u_i(t_k^i) = \left(u_i(t_k^i|t_k^i), \ldots, u_i(t_k^i + T|t_k^i) \right)$ denotes the input sequence for quadrotor i.

The local stage cost of quadrotor i is designed as:

$$L_i(s|t_k^i) = ||u_i(s|t_k^i)||_P^2 + ||\xi_i(s|t_k^i) - \xi_{i,r}(s|t_k^i)||_Q^2$$

The local terminal cost is designed as $g_i(\xi_i(t_k^i + T|t_k^i)) = ||\xi_i(t_k^i + T|t_k^i)||_R^2$, where the weighting matrices P, Q, and R are all symmetric and positive definite. Additionally, the formation composition and keeping of quadrotors are achieved based on the coupling cost term $||\xi_i(s|t_k^i) - \xi_{i,r}(s|t_k^i)||_Q^2$.

3.2 | Disturbance-based EDMPC design

In this section, an ETM is applied to a quadrotor system, aiming to reduce the computational load on the onboard device and determine the next time t_{k+1}^i for solving an optimization problem. This mechanism operates on the principle of identifying the discrepancy between the actual trajectory and the optimally predicted trajectory. Recalculating the control input sequence is imperative once the discrepancy exceeds the predefined threshold. To formulate the ETM, a time instant $\hat{t}_{k+1}^i$ is defined as:

$$\hat{t}_{k+1}^i \triangleq \inf_{s > t_k^i} \left\{ s : ||\bar{\xi}_i\left(s|t_k^i\right) - \xi_i\left(s|t_k^i\right)|| > \mathcal{O} \right\} \tag{7}$$

where $s \in (t_k^i, t_k^i + T)$, $\mathcal{O} = \bar{\omega}\zeta T e^{L_p \zeta T}$ is trigger level, $\zeta \in (0, 1)$ is an adjustment parameter, L_p is tepshe Lipschitz constant, and $\bar{\omega}$ is the disturbance bound. It is assumed that the optimization problem is automatically initiated at the initial time t_0. Additionally, the ETM is activated at each time instant. Define the iteration interval $H^i(t_k^i) = T$. This means that the error between the actual state and the optimal state of the quadrotor within the prediction time has not reached the threshold. Then, the optimal control sequence is fully executed. Thus, the triggering time t_{k+1}^i is defined as:

$$t_{k+1}^i = \min\{\hat{t}_{k+1}^i, t_k^i + T\} \tag{8}$$

Theorem 1. Consider that the quadrotor system (4) with Assumptions 1-4 are satisfied and the triggered mechanisms (7) and (8) are employed. Then, the lower and upper bounds of the event-triggered inter-execution time are given by $\inf_{k\in\mathbb{N}}\{t^i_{k+1}-t^i_k \geq \zeta T\}$ and $\sup_{k\in\mathbb{N}}\{t^i_{k+1}-t^i_k \leq T\}$, respectively.

Proof. The upper bound of the inter-execution time directly follows from (8). To prove the result on the lower bound, $||\xi_i(s) - \xi^*_i(s)||$ is considered at the time instant t^i_k. By applying the triangle inequality, $||\xi_i(s) - \xi^*_i(s|t^i_k)|| \leq \bar{\omega}(s - t^i_k) + L_p \int^s_{t^i_k} ||\xi_i(t) - \xi^*_i(t|t^i_k)||dt$ is obtained. By using the Gronwall–Bellman inequality, it is derived that $||\xi_i(s) - \xi^*_i(s|t^i_k)|| \leq \bar{\omega}(s - t^i_k)e^{L_p(s-t^i_k)}$. According to (7), $t^i_{k+1} \geq t^i_k + \zeta T$ is obtained. By using (8), it follows that $\inf_{k\in\mathbb{N}}\{t^i_{k+1} - t^i_k \geq \zeta T\}$. The proof is completed. $\square$

The aforementioned ETM is deployed to each quadrotor to implement the EDMPC algorithm. For quadrotor i at t^i_k, the optimization problem $\mathcal{K}_i(t^i_k)$ to be solved is formulated as:

$$\min_{u_i(s|t_k)} J_i(t^i_k) = J_i(\xi_i(t^i_k), \xi_{i,r}(t^i_k), u_i(t^i_k)) \tag{9}$$

$$\text{s.t.} \quad \begin{aligned} &\xi_i(0|t^i_k) = \xi_i(t^i_k), \\ &||\xi_i((s|t_k))|| \leq \frac{\varepsilon T}{s - t_k}, \\ &u_i(s|t^i_k) \in \mathcal{U}, \\ &\dot{\xi}_i(s|t^i_k) = f_i(\xi_i(s|t^i_k), u_i(s|t^i_k)), \\ &||\xi_i(s|t^i_k) - \xi^b_i(s + t^i_k - t^i_{k-1}|t^i_{k-1})|| \leq \Delta_i, \\ &\xi_i(t_k + T|t_k) \in \Omega_\epsilon. \end{aligned} \tag{10}$$

where $\Omega_\epsilon = \left\{\xi_i(t^i_k + T) : ||\xi_i(t^i_k + T)|| \leq \epsilon\right\}$ as the terminal region. The term $\Delta_i = \mathcal{O}L_p^{T-\zeta T}$ is a designed parameter and $\mathcal{U}$ is the control input constraint. The proposed event-triggered asynchronous DMPC method is concisely delineated in Algorithm 1.

Remark 1. It is imperative to emphasize that the system involved in the optimization problem (9) is presumed to be nominal, implying that the model within the controller remains undisturbed. By resolving the optimization problem $\mathcal{K}_i(t^i_k)$ subject to (10) over the interval $s \in (t^i_k, t^i_k + T]$, it is possible to ascertain the optimal predictive control sequence $u^*_i(s|t^i_k)$ and the corresponding optimal state $\xi^*_i(s|t^i_k)$. However, due to the deployment of the EDMPC strategy by each quadrotor, which is subject to different disturbances, resulting in asynchronous communication instants, the effects caused by communication delays are amplified. Hence, to ensure that multi-quadrotor systems can complete tasks with high precision in such a complex environment, recursive feasibility and stability analysis must be conducted.

4 | FEASIBILITY AND STABILITY ANALYSIS

To evaluate the feasibility of the EDMPC strategy and confirm the stability of multi-quadrotor systems, the analysis commences with the formulation of a local feedback controller $u^\kappa_i = [U_{i,1_{\kappa_f}}, U_{i,2_{\kappa_f}}, U_{i,3_{\kappa_f}}, U_{i,4_{\kappa_f}}]^T$ and the establishment of a terminal region Ω for the nominal quadrotor system of the followers. The terminal region $\Omega = \left\{\xi_i(s|t^i_k) : ||\xi_i(s|t^i_k)|| \leq r\right\}$ for the nominal system is selected to maintain invariance through the application of the local control law u^κ_i. Thereafter, a robust terminal region $\Omega_\epsilon \subseteq \Omega$ is used to address disturbances in multi-quadrotor systems. In the end, the proposed algorithm is analyzed for recursive feasibility and stability based on two types of communication delay scenarios.

4.1 | Feasibility analysis

Theorem 2. Consider the quadrotor system described by (4), and suppose that the optimization problem solver is triggered by mechanism (7), and the triggering time is defined as (8). By implementing the EDMPC scheme, the optimization problem (9) under constraints (10) is recursively feasible when the following two conditions are satisfied.

(1) The optimization problem (9) can be solved at the initial time t_0 with zero communication delay.

(2) The upper bound of disturbance $\bar{\omega}$ and positive constants δ exist such that $\bar{\omega} \leq \frac{e^{-L_p T}}{\delta}(r - \epsilon)$, $\delta \geq \frac{1}{L_p}\ln\frac{r}{\epsilon}$ and $\beta r \leq \epsilon < r$, where $\delta = \zeta T$ and $\beta = \frac{T-\delta}{T}$.

Algorithm 1 Event-triggered asynchronous DMPC algorithm

Require: For quadrotor i, $i \in \mathcal{M}$, the weighting matrices P, Q, R, the prediction horizon N, the sampling period Δt, the terminal set Ω, the parameter Δ_i, the initial state $\xi_i(t_k^i)$, and other related parameters. Set $k = 0$, $t_k^i = 0$.

1: **while** The control action is not stopped **do**
2:    **if** Update condition (7) is triggered **then**
3:       Solve Problem $\mathcal{K}_i(t_k^i)$ and sample local system state;
4:       **if** Obtain neighboring quadrotors information **then**
5:          Update the predicted state sequence $\xi_j^b(s|t_k^j)$;
6:       **else**
7:          Use the historical predicted state sequence $\xi_j^b(s|t_{k-1}^j)$;
8:       **end if**
9:       Construct the state sequence $\xi_{i,r}(s|t_k^j)$ as in (6);
10:      Solve the Problem $\mathcal{K}_i(t_k^i)$ to generate $u_i^*(s|t_k^i)$;
11:      Broadcast $\xi_i^b(s|t_k^i)$ as in (5) to its neighbors;
12:      Apply the first input in the control sequence $u_i^*(s|t_k^i)$ to quadrotor i and update the control sequence;
13:      $k = k + 1$;
14:    **else**
15:      Apply the optimal historical input in the control sequence $u_i^*(s|t_k^i)$ to quadrotor i and update the control sequence;
16:    **end if**
17: **end while**

Proof. At time t_k^i, the optimal solution for problem $\mathcal{K}_i(t_k^i)$ is $u_i^*(t_k^i) = \{u_i^*(t_k^i|t_k^i), u_i^*(t_k^i + \Delta t|t_k^i), \ldots, u_i^*(t_k^i + T|t_k^i)\}$, corresponding to the optimal state trajectory of the system $\xi_i^*(t_k^i) = \{\xi_i^*(t_k^i|t_k^i), \xi_i^*(t_k^i + \Delta t|t_k^i), \ldots, \xi_i^*(t_k^i + T|t_k^i)\}$. All components of the aforementioned optimal solution and corresponding state trajectory satisfy the constraint conditions (10). At time t_{k+1}^i, the solution to problem $\mathcal{K}_i(t_k^i)$ is constructed as:

$$\bar{u}_i(s|t_{k+1}^i) = \begin{cases} u_i^*(s|t_k^i), s \in [t_{k+1}^i, t_k^i + T) \\ u_i^\kappa(s|t_k^i), s \in [t_k^i + T, t_{k+1}^i + T] \end{cases} \tag{11}$$

Consider the time interval $s \in [t_{k+1}^i, t_k^i + T)$. The difference between the feasible states $\bar{\xi}_i(s|t_{k+1}^i)$ and the optimal states $\xi_i^*(s|t_k^i)$ satisfies:

$$||\bar{\xi}_i(s|t_{k+1}^i) - \xi_i^*(s|t_k^i)||$$

$$= ||\xi_i(t_{k+1}^i) - \xi_i(t_{k+1}^i|t_k^i) - L_p \int_{t_{k+1}^i}^{\gamma} ||\bar{\xi}_i(s|t_{k+1}^i) - \xi_i^*(s|t_k^i)||d\gamma$$

$$\leq \mathcal{O} + L_p \int_{t_{k+1}^i}^{\gamma} ||\bar{\xi}_i(s|t_{k+1}^i) - \xi_i^*(s|t_k^i)||d\gamma$$

$$\leq \mathcal{O}e^{L_p(s - t_{k+1}^i)} \tag{12}$$

Substitute the time instant $s = t_k^i + T$ and $\mathcal{O} = \bar{\omega}\delta e^{L_p\delta}$, where $\delta = \zeta T$. The following expression is obtained:

$$||\bar{\xi}_i(t_k^i + T|t_{k+1}^i)|| \leq ||\xi_i^*(t_k^i + T|t_k^i)|| + \bar{\omega}\delta e^{L_p T} \tag{13}$$

Since $||\xi_i^*(t_k^i + T|t_k)|| \leq \epsilon$ and $\bar{\omega} \leqslant \frac{e^{-L_p T}}{\delta}(r - \epsilon)$, the following expression is obtained:

$$||\bar{\xi}_i(t_k^i + T|t_{k+1}^i)|| \leq r \tag{14}$$

which infers that $\bar{\xi}_i(t_k^i + T|t_{k+1}^i) \in \Omega$ holds. Subsequently, to demonstrate the validity of the state constraint within the interval $s \in [t_{k+1}^i, t_k^i + T)$ from (12), the following expression can be derived:

$$||\bar{\xi}_i(s|t_{k+1}^i)|| \leq \frac{\epsilon T}{s - t_k^i} + (r - \epsilon) \tag{15}$$

One has that $r - \epsilon \leqslant \frac{\delta}{T-\delta}\epsilon \leqslant \frac{t^i_{k+1}-t^i_k}{(s-t^i_k)(s-t^i_{k+1})}T\epsilon$. By substituting this condition to (15), the following expression is derived:

$$||\bar{\bar{\xi}}_i(s|t^i_{k+1})|| \leq \frac{T}{s-t^i_{k+1}}\epsilon \tag{16}$$

Hence, it can be concluded that the controller (11) can drive the terminal state into the set Ω_ϵ. By mathematical induction, this ensures that the optimization problem $\mathcal{K}_i(t^i_k)$ has an iterative feasibility at every triggering moment t^i_k. □

4.2 | Stability analysis

Theorem 3. The multi-quadrotor systems employing the proposed EDMPC scheme are input-state practical stable (ISpS) under communication delays when constant $l > 0$ is satisfied, where $l = 4\underline{\lambda}(Q)\epsilon^2 - \frac{2\bar{\lambda}(Q)\bar{\omega}(2\epsilon+\alpha)}{\sqrt{2}L_p}(\frac{T^2}{\delta} - T)^{\frac{1}{2}}(e^{2L_pT} - e^{2L_p\delta})^{\frac{1}{2}} - \frac{\bar{\lambda}(Q)\bar{\omega}^2\delta}{2L_p}(e^{2L_pT} - e^{2L_p\delta}) - (3r+\epsilon)\bar{\lambda}(R)\bar{\omega}e^{L_pT} - (\bar{\lambda}(Q)(T-\delta) + \bar{\lambda}(R))\bar{\omega}^2e^{2L_p\delta}L_p^{2(T-\delta)}\delta - 2\bar{\omega}e^{L_p\delta}L_p^{T-\delta}((\alpha(T-\delta) + 2\epsilon T\ln(\frac{T}{\delta}))\bar{\lambda}(Q) + 2\epsilon\bar{\lambda}(R))$.

The formation error finally converges to the set $\mathbb{S}$ as follows:

$$\mathbb{S} = \{\xi_i - \xi_{i,r} : ||\xi_i - \xi_{i,r}||^2 \leq \bar{\omega}^2\delta^2e^{2L_p\delta} + 2\epsilon\bar{\omega}\delta e^{L_p\delta} + \frac{1}{\underline{\lambda}(Q)}(\frac{2\bar{\lambda}(Q)\bar{\omega}\epsilon}{L_p}(e^{L_pT} - e^{L_p\delta}) + \frac{\bar{\lambda}(Q)\bar{\omega}^2\delta}{2L_p}(e^{2L_pT} - e^{2L_p\delta})$$

$$+ \frac{2\bar{\lambda}(Q)\bar{\omega}(\epsilon + \alpha)}{\sqrt{2}L_p}(\frac{T^2}{\delta} - T)^{\frac{1}{2}}(e^{2L_pT} - e^{2L_p\delta})^{\frac{1}{2}} + (3r+\epsilon)\bar{\lambda}(R)\bar{\omega}e^{L_pT} + (\bar{\lambda}(Q)(T-\delta)$$

$$+ \bar{\lambda}(R))\bar{\omega}^2e^{2L_p\delta}L_p^{2(T-\delta)}\delta + 2\bar{\omega}e^{L_p\delta}L_p^{T-\delta}((\alpha(T-\delta) + 2\epsilon T\ln(\frac{T}{\delta}))\bar{\lambda}(Q) + 2\epsilon\bar{\lambda}(R))))\} \tag{17}$$

where $\bar{\lambda}(Q)$ and $\underline{\lambda}(Q)$ denote the largest and smallest eigenvalues of the matrix Q.

Proof. Select a Lyapunov function:

$$V(t_k) = J(\xi^*_i(t^i_k), u^*_i(t^i_k)) \tag{18}$$

Consider the difference in the values of the Lyapunov function at t^i_k and t^i_{k+1},

$$\Delta V = V(t^i_{k+1}) - V(t^i_k) \leq J(\bar{\xi}_i(t^i_{k+1}), \bar{u}_i(t^i_{k+1})) - J(\xi^*_i(t^i_k), u^*_i(t^i_k)) \tag{19}$$

According to $\bar{u}_i(s|t^i_{k+1}) = u^*_i(s|t^i_k)$, split the terms (19) into $\Delta V = \sum_{i=1}^3 \Delta V_i$, such that $\Delta V_i, i = 1, 2, 3$ as follows:

$$\Delta V_1 = \int_{t^i_{k+1}}^{t^i_k+T} \left(||\bar{\xi}_i(s|t^i_{k+1}) - \xi_{i,r}(s|t^i_{k+1})||^2_Q - ||\xi^*_i(s|t^i_k) - \xi_{i,r}(s|t^i_k)||^2_Q \right) ds \tag{20}$$

$$\Delta V_2 = \int_{t^i_k+T}^{t^i_{k+1}+T} \left((||\bar{\xi}_i(s|t^i_{k+1}) - \xi_{i,r}(s|t^i_{k+1})||^2_Q + ||\bar{u}_i(s|t^i_{k+1})||^2_P \right) ds + ||\bar{\xi}_i(t^i_{k+1} + T|t^i_{k+1})||^2_R - ||\xi^*_i(t^i_k + T|t_k)||^2_R \tag{21}$$

$$\Delta V_3 = -\int_{t^i_k}^{t^i_{k+1}} \left(||\xi^*_i(s|t^i_k) - \xi_{i,r}(s|t^i_k)||^2_Q + ||u^*_i(s|t^i_k)||^2_P \right) ds \tag{22}$$

The scenario where $||\xi_i(t^i_k|t^i_k)|| \geq \epsilon$ and time-varying communication delays in **CASE 1** are considered first. In this case, the predicted states of neighbors transmitted at the previously triggering time instant $\xi^b_j(t^i_{k+1}) = (\xi^b_j(H^i + t^i_k|t^i_k), \cdots, \xi^b_j(H^i + t^i_k + T|t^i_k))$ will be used. For ΔV_1, the following expression can be derived:

$$\Delta V_1 \leq \int_{t^i_{k+1}}^{t^i_k+T} ((||\bar{\xi}_i(s|t^i_{k+1}) - \xi^*_i(s|t^i_k)||_Q) \times ((||\bar{\xi}_i(s|t^i_{k+1})||_Q + ||\xi^*_i(s|t^i_k)||_Q + 2||\xi_{i,r}(s|t^i_k)||_Q))ds \tag{23}$$

According to term (5) and **Theorem 2**, it is known that $||\xi^b_j(s|t^i_k)|| < r$. Furthermore, based on (7), it can be inferred that $\xi_i(s|t^i_k) - \xi^*_i(s|t^i_k) \leq \mathcal{O}$. By substituting this result and employing the triangle inequality and Hölder's inequality, the following

expression can be derived:

$$\Delta V_1 \leq \int_{t^i_{k+1}}^{t^i_k+T} [\bar{\lambda}(Q)\bar{\omega}\delta e^{L_p(s+\delta-t^i_{k+1})}(2||\xi^*_i(s|t^i_k)|| + \bar{\omega}\delta e^{L_p(s+\delta-t^i_{k+1})} + 2||\xi_{i,r}(s|t^i_k)||)]ds$$

$$\leq (\int_{t^i_{k+1}}^{t^i_k+T} ||\xi^*_i(s|t^i_k)||^2 + ||\xi_{i,r}(s|t^i_k)||^2 ds)^{\frac{1}{2}} \times \frac{2\bar{\lambda}(Q)\bar{\omega}\delta}{\sqrt{2}L_p}(e^{2L_pT} - e^{2L_p\delta})^{\frac{1}{2}} + \frac{\bar{\lambda}(Q)\bar{\omega}^2\delta^2}{2L_p}(e^{2L_pT} - e^{2L_p\delta})$$

$$\leq \frac{2\bar{\lambda}(Q)\bar{\omega}\delta(2\epsilon+\alpha)}{\sqrt{2}L_p}(\frac{T^2}{\delta} - T)^{\frac{1}{2}}(e^{2L_pT} - e^{2L_p\delta})^{\frac{1}{2}} + \frac{\bar{\lambda}(Q)\bar{\omega}^2\delta^2}{2L_p}(e^{2L_pT} - e^{2L_p\delta}) \tag{24}$$

For ΔV_2, after taking the derivative concerning constraint (10) and substituting, the following expression can be derived:

$$\Delta V_2 \leq ||\bar{\xi}_i(t^i_k + T|t^i_{k+1}) - \xi_{i,r}(t^i_k + T|t^i_k)||^2_R - ||\xi^*_i(t^i_k + T|t^i_k) - \xi_{i,r}(t^i_k + T|t^i_k)||^2_R$$

$$\leq \bar{\lambda}(R)(||\bar{\xi}_i(t^i_k + T|t^i_{k+1}) - \xi^*_i(t^i_k + T|t^i_k)||) \times ((||\bar{\xi}_i(t^i_k + T|t^i_{k+1})|| + ||\xi^*_i(t^i_k + T|t^i_k)|| + 2||\xi_{i,r}(t^i_k + T|t^i_k)||))$$

$$\leq (3r + \epsilon)\bar{\lambda}(R)\bar{\omega}\delta e^{L_pT} \tag{25}$$

For ΔV_3, $||\bar{\xi}(t^i_{k+1}|t^i_k)|| > \epsilon$ is considered. This indicates that for $s \in [t^i_k, t^i_{k+1})$, $||\bar{\xi}(s|t^i_k)|| > \epsilon$, the following expression can be derived:

$$\Delta V_3 \leq - \int_{t^i_k}^{t^i_{k+1}} ||\xi^*_i(s|t^i_k) - \xi_{i,r}(s|t^i_k)||^2_Q ds \leq -4\underline{\lambda}(Q)\delta\epsilon^2 \tag{26}$$

For $\Delta V = \sum_{i=1}^3 \Delta V_i$, the following expression can be derived:

$$\Delta V \leq \frac{2\bar{\lambda}(Q)\bar{\omega}\delta(2\epsilon+\alpha)}{\sqrt{2}L_p}(\frac{T^2}{\delta} - T)^{\frac{1}{2}}(e^{2L_pT} - e^{2L_p\delta})^{\frac{1}{2}} + \frac{\bar{\lambda}(Q)\bar{\omega}^2\delta^2}{2L_p}(e^{2L_pT} - e^{2L_p\delta})$$

$$+ (3r + \epsilon)\bar{\lambda}(R)\bar{\omega}\delta e^{L_pT} - 4\underline{\lambda}(Q)\delta\epsilon^2 \tag{27}$$

According to equation (27), $\Delta V < -l\delta$ is obtained. Let $\mu = \frac{V(0)-\delta\ell}{V(0)}$, $V(t^i_{k+1}) < \mu V(t^i_k)$, where $\mu \in (0, 1)$ as a decreasing rate. This implies that the multi-quadrotor systems asymptotically converge to the desired velocity and desired formation within a finite time. When the state enters the terminal set, i.e., $\xi(t^i_k|t^i_k) \in \Omega_\epsilon$, ΔV_1 are re-scaled as:

$$\Delta V_1 \leq \int_{t^i_{k+1}}^{t^i_k+T} [\bar{\lambda}(Q)\bar{\omega}\delta e^{L_p(s+\delta-t^i_{k+1})}(2||\bar{\xi}_i(s|t^i_k)|| + \bar{\omega}\delta e^{L_p(s+\delta-t^i_{k+1})} + 2||\xi_{i,r}(s|t^i_k)||)]ds$$

$$\leq \frac{2\bar{\lambda}(Q)\bar{\omega}\delta(\epsilon)}{L_p}(e^{L_pT} - e^{L_p\delta}) + \frac{\bar{\lambda}(Q)\bar{\omega}^2\delta^2}{2L_p}(e^{2L_pT} - e^{2L_p\delta}) + \frac{2\bar{\lambda}(Q)\bar{\omega}\delta(\epsilon+\alpha)}{\sqrt{2}L_p}(\frac{T^2}{\delta} - T)^{\frac{1}{2}}(e^{2L_pT} - e^{2L_p\delta})^{\frac{1}{2}} \tag{28}$$

For ΔV_3, suppose that the local controller $u^\kappa_i(s|t^i_k)$ is applied to the system. Then, $||\xi^*_i(s|t^i_k) - \xi_{i,r}(s|t^i_k)||_Q$ obviously decreases with respect to time s. Furthermore, since $u^\kappa_i(s|t^i_k)$ is an optimal solution, the following expression can be derived:

$$\Delta V_3 \leq - \int_{t^i_k}^{t^i_{k+1}} (||\xi^*_i(s|t^i_k) - \xi_{i,r}(s|t^i_k)||^2_Q + ||u^*_i(s|t^i_k)||^2_P)ds$$

$$\leq -\underline{\lambda}(Q)\delta||\xi^*_i(t^i_{k+1}|t^i_k) - \xi_{i,r}(t^i_{k+1}|t^i_k)||^2$$

$$\leq -\underline{\lambda}(Q)\delta||\xi_i(t^i_{k+1}) - \xi_{i,r}(t^i_{k+1}|t^i_k)||^2 + \underline{\lambda}(Q)\bar{\omega}^2\delta^3 e^{2L_p\delta} + 2\underline{\lambda}(Q)\epsilon\bar{\omega}\delta^2 e^{L_p\delta} \tag{29}$$

The summation $\Delta V = \sum_{i=1}^{3} \Delta V_i$ yields the following expression:

$$\Delta V \leq \frac{2\bar{\lambda}(Q)\bar{\omega}\delta\epsilon}{L_p}(e^{L_p T} - e^{L_p \delta}) + \frac{\bar{\lambda}(Q)\bar{\omega}^2\delta^2}{2L_p}(e^{2L_p T} - e^{2L_p \delta}) + \frac{2\bar{\lambda}(Q)\bar{\omega}\delta(\epsilon + \alpha)}{\sqrt{2}L_p}(\frac{T^2}{\delta} - T)^{\frac{1}{2}}(e^{2L_p T} - e^{2L_p \delta})^{\frac{1}{2}}$$

$$- \underline{\lambda}(Q)\delta||\xi_i(t_{k+1}^i) - \xi_{i,r}(t_{k+1}^i|t_k^i)||^2 + \underline{\lambda}(Q)\bar{\omega}^2\delta^3 e^{2L_p\delta} + 2\underline{\lambda}(Q)\epsilon\bar{\omega}\delta^2 e^{L_p\delta} + (3r + \epsilon)\bar{\lambda}(R)\bar{\omega}\delta e^{L_p T}$$

$$\leq -\underline{\lambda}(Q)\delta||\xi_i(t_{k+1}^i) - \xi_{i,r}(t_{k+1}^i|t_k^i)||^2 + F(\bar{\omega}) \tag{30}$$

where $F(\bar{\omega}) = \frac{2\bar{\lambda}(Q)\bar{\omega}\delta\epsilon}{L_p}(e^{L_p T} - e^{L_p \delta}) + \frac{\bar{\lambda}(Q)\bar{\omega}^2\delta^2}{2L_p}(e^{2L_p T} - e^{2L_p \delta}) + \frac{2\bar{\lambda}(Q)\bar{\omega}\delta(\epsilon+\alpha)}{\sqrt{2}L_p}(\frac{T^2}{\delta} - T)^{\frac{1}{2}}(e^{2L_p T} - e^{2L_p \delta})^{\frac{1}{2}} + (3r + \epsilon)\bar{\lambda}(R)\bar{\omega}\delta e^{L_p T} + \underline{\lambda}(Q)\bar{\omega}^2\delta^3 e^{2L_p\delta} + 2\underline{\lambda}(Q)\epsilon\bar{\omega}\delta^2 e^{L_p\delta}$. It is a class of K-class functions concerning $\bar{\omega}$. Subsequently, the case is considered where $||\xi_i^*(s|t_k)|| \geq \epsilon$ and time-varying communication delays in **CASE 2**. The latest predicted states of neighbors, denoted as $\xi_j^b(t_{k+1}^i) = (\xi_j^b(t_{k+1}^i|t_{k+1}^i), \ldots, \xi_j^b(t_{k+1}^i + T|t_{k+1}^i))$, will be received and used by quadrotor i. For ΔV_1, applying the consistency constraint (10) and triangle inequality, the following relationship is established:

$$||\xi_i(s|t_{k+1}^i) - \xi_{i,r}(s|t_{k+1}^i)||_Q^2 \leq ||\xi_i(s|t_k^i) - \xi_{i,r}(s|t_k^i)||_Q^2 + 2||\xi_i(s|t_k^i) - \xi_{i,r}(s|t_k^i)||\bar{\lambda}(Q)\Delta_j + \bar{\lambda}(Q)\Delta_j^2. \tag{31}$$

where $\Delta_j = \bar{\omega}\delta e^{L_p\delta}L_p^{T-\delta}$.

For ΔV_1, the following expression is obtained:

$$\Delta V_1 \leq \int_{t_{k+1}^i}^{t_k^i + T} (||\xi_i(s|t_{k+1}^i) - \xi_{i,r}(s|t_k^i)||_Q^2 - ||\xi_i^*(s|t_k^i) - \xi_{i,r}(s|t_k^i)||_Q^2) \, ds$$

$$+ (\alpha(T - \delta) + 2\epsilon T \ln(\frac{T}{\delta}))\bar{\lambda}(Q)\Delta_j + (T - \delta)\bar{\lambda}(Q)\Delta_j^2$$

$$\leq \frac{2\bar{\lambda}(Q)\bar{\omega}\delta(2\epsilon + \alpha)}{\sqrt{2}L_p}(\frac{T^2}{\delta} - T)^{\frac{1}{2}}(e^{2L_p T} - e^{2L_p \delta})^{\frac{1}{2}} + \frac{\bar{\lambda}(Q)\bar{\omega}^2\delta^2}{2L_p}(e^{2L_p T} - e^{2L_p \delta})$$

$$+ (\alpha(T - \delta) + 2\epsilon T \ln(\frac{T}{\delta}))\bar{\lambda}(Q)\Delta_j + (T - \delta)\bar{\lambda}(Q)\Delta_j^2 \tag{32}$$

For ΔV_2, after taking the derivative concerning constraint (10) and substituting, the result can be expressed as:

$$\Delta V_2 \leq ||\bar{\xi}_i(t_k^i + T|t_{k+1}^i) - \xi_{i,r}(t_k^i + T|t_{k+1}^i)||_R^2 - ||\xi_i^*(t_k^i + T|t_k^i) - \xi_{i,r}(t_k^i + T|t_k^i)||_R^2$$

$$\leq ||\bar{\xi}_i(t_k^i + T|t_{k+1}^i) - \xi_{i,r}(t_k^i + T|t_k^i)||_R^2 - ||\xi_i^*(t_k^i + T|t_k^i) - \xi_{i,r}(t_k^i + T|t_k^i)||_R^2$$

$$+ 2\epsilon\bar{\lambda}(R)\Delta_j + \bar{\lambda}(R)\Delta_j^2$$

$$\leq (3r + \epsilon)\bar{\lambda}(R)\bar{\omega}\delta e^{L_p T} + 2\epsilon\bar{\lambda}(R)\Delta_j + \bar{\lambda}(R)\Delta_j^2 \tag{33}$$

For ΔV_3, the result can be expressed as:

$$\Delta V_3 \leq -4\underline{\lambda}(Q)\delta\epsilon^2 \tag{34}$$

It follows from the results of (32), (33), and (34) that the following expression is obtained:

$$\Delta V \leq \frac{2\bar{\lambda}(Q)\bar{\omega}\delta(2\epsilon + \alpha))}{\sqrt{2}L_p}(\frac{T^2}{\delta} - T)^{\frac{1}{2}}(e^{2L_p T} - e^{2L_p \delta})^{\frac{1}{2}} + \frac{\bar{\lambda}(Q)\bar{\omega}^2\delta^2}{2L_p}(e^{2L_p T} - e^{2L_p \delta})$$

$$+ (3r + \epsilon)\bar{\lambda}(R)\bar{\omega}\delta e^{L_p T} - 4\underline{\lambda}(Q)\delta\epsilon^2 + (\alpha(T - \delta) + 2\epsilon T \ln(\frac{T}{\delta}))\bar{\lambda}(Q)\Delta_j$$

$$+ (T - \delta)\bar{\lambda}(Q)\Delta_j^2 + 2\epsilon\bar{\lambda}(R)\Delta_j + \bar{\lambda}(R)\Delta_j^2 \tag{35}$$

According to (35), $\Delta V < -l\delta$ is obtained, i.e., $V(t_{k+1}^i) < V(t_k^i) - l\delta$. Let $\mu = \frac{V(0) - \delta\ell}{V(0)}$. Subsequently, $V(t_{k+1}^i) < \mu V(t_k^i)$ is derived. This implies that the multi-quadrotor systems asymptotically converge to the desired velocity and desired formation within a finite time. When the state enters the terminal set, i.e., $\xi^*(t_k^i|t_k^i) \in \Omega_\epsilon$, the re-scaling of ΔV_1 and ΔV_3 can be performed:

$$\Delta V_1 \leq \frac{2\bar{\lambda}(Q)\bar{\omega}\delta\epsilon}{L_p}(e^{L_p T} - e^{L_p \delta}) + \frac{2\bar{\lambda}(Q)\bar{\omega}\delta(\epsilon + \alpha)}{\sqrt{2}L_p}(\frac{T^2}{\delta} - T)^{\frac{1}{2}}(e^{2L_p T} - e^{2L_p \delta})^{\frac{1}{2}}$$

$$+ (\alpha(T - \delta) + 2\epsilon T \ln(\frac{T}{\delta}))\bar{\lambda}(Q)\Delta_j + (T - \delta)\bar{\lambda}(Q)\Delta_j^2 + \frac{\bar{\lambda}(Q)\bar{\omega}^2\delta^2}{2L_p}(e^{2L_p T} - e^{2L_p \delta}) \tag{36}$$

$$\Delta V_3 \leq -\underline{\lambda}(Q)\delta||\xi_i(t^i_{k+1}) - \xi_{i,r}(t^i_{k+1}|t^i_k)||^2 + \bar{\lambda}(Q)\bar{\omega}^2\delta^3 e^{2L_p\delta} + 2\underline{\lambda}(Q)\epsilon\bar{\omega}\delta^2 e^{L_p\delta} \tag{37}$$

According to $\Delta V = \sum_{i=1}^3 \Delta V_i$, the result can be expressed as:

$$
\begin{aligned}
\Delta V \leq &\frac{2\bar{\lambda}(Q)\bar{\omega}\delta\epsilon}{L_p}(e^{L_pT} - e^{L_p\delta}) + \frac{\bar{\lambda}(Q)\bar{\omega}^2\delta^2}{2L_p}(e^{2L_pT} - e^{2L_p\delta}) + (T-\delta)\bar{\lambda}(Q)\Delta_j^2 + \frac{2\bar{\lambda}(Q)\bar{\omega}\delta(\epsilon+\alpha)}{\sqrt{2}L_p}(\frac{T^2}{\delta} - T)^{\frac{1}{2}}(e^{2L_pT} - e^{2L_p\delta})^{\frac{1}{2}} \\
&+ (3r+\epsilon)\bar{\lambda}(R)\bar{\omega}\delta e^{L_pT} + 2\epsilon\bar{\lambda}(R)\Delta_j + \bar{\lambda}(R)\Delta_j^2 + (\alpha(T-\delta) + 2\epsilon T\ln(\frac{T}{\delta}))\bar{\lambda}(Q)\Delta_j \\
&- \underline{\lambda}(Q)\delta||\xi_i(t^i_{k+1}) - \xi_{i,r}(t^i_{k+1}|t^i_k)||^2 + \bar{\lambda}(Q)\bar{\omega}^2\delta^3 e^{2L_p\delta} + 2\underline{\lambda}(Q)\epsilon\bar{\omega}\delta^2 e^{L_p\delta} \\
\leq &-\underline{\lambda}(Q)\delta||\xi_i(t^i_{k+1}) - \xi_{i,r}(t^i_{k+1}|t^i_k)||^2 + G(\bar{\omega}) \tag{38}
\end{aligned}
$$

where $G(\bar{\omega}) = \frac{2\bar{\lambda}(Q)\bar{\omega}\delta\epsilon}{L_p}(e^{L_pT} - e^{L_p\delta}) + \frac{\bar{\lambda}(Q)\bar{\omega}^2\delta^2}{2L_p}(e^{2L_pT} - e^{2L_p\delta}) + \frac{2\bar{\lambda}(Q)\bar{\omega}\delta(\epsilon+\alpha)}{\sqrt{2}L_p}(\frac{T^2}{\delta} - T)^{\frac{1}{2}}(e^{2L_pT} - e^{2L_p\delta})^{\frac{1}{2}} + (T-\delta)\bar{\lambda}(Q)\Delta_j^2 + (3r+\epsilon)\bar{\lambda}(R)\bar{\omega}\delta e^{L_pT} + 2\epsilon\bar{\lambda}(R)\Delta_j + \bar{\lambda}(R)\Delta_j^2 + (\alpha(T-\delta) + 2\epsilon T\ln(\frac{T}{\delta}))\bar{\lambda}(Q)\Delta_j + \bar{\lambda}(Q)\bar{\omega}^2\delta^3 e^{2L_p\delta} + 2\underline{\lambda}(Q)\epsilon\bar{\omega}\delta^2 e^{L_p\delta}$. This implies that the quadrotor system is ISpS, and the states of the formation error converge to the set Ω. Therefore, the proofs for the two cases of communication delays are completed. $\square$

Remark 2. A novel EDMPC scheme is proposed by combining ETM, DMPC, and innovative information transmission strategies. A rigorous theoretical analysis of the recursive feasibility and ISpS of the entire multi-quadrotor systems is presented. The proposed EDMPC scheme ensures that the formation error of quadrotors converges to a small region around zero in finite time, even in the presence of additive disturbances and communication delays. The focus or challenge lies in ensuring the accuracy and stability of the formation composition and keeping performance of the multi-quadrotor systems in the presence of various communication delays.

5 | SIMULATION RESULTS

In this section, numerical and SIL simulations of the EDMPC method are provided to demonstrate the effectiveness of the multi-quadrotor systems with communication delays. The multi-quadrotor systems consist of one leader quadrotor and four follower quadrotors, all of which have the same structure, with detailed parameters listed in TABLE 1. Quadrotor 1 is tasked with trajectory tracking and instruction acquisition. Figure 1 illustrates the communication topology graph, denoted as $\mathcal{G}$. Arrows in the figure represent the information flow, signifying that the front-end quadrotor's broadcasted information must be acquired by the rear-end quadrotors. The leader's reference trajectory is predefined as follows:

$$
\begin{aligned}
x_{ref} &= 10(\sin(0.1t) - (\sin(0.1t))^3) \\
y_{ref} &= 10(\cos(0.1t) - (\cos(0.1t))^3) \\
z_{ref} &= 5 + \sin(0.1t) \\
\psi_{ref} &= 0
\end{aligned}
$$

According to the predefined mission requirements, the initial and relative positions of the subsequent quadrotors to the leader quadrotor in the Frenet-Serret coordinate system must align with the values specified in TABLE 2.

TABLE 1 Quadrotor Parameters Table

Parameter	Value	Unit	Description
I_{xx}	0.456	$kg \cdot m^2$	Moment of inertia (about x-axis)
I_{yy}	0.456	$kg \cdot m^2$	Moment of inertia (about y-axis)
I_{zz}	0.641	$kg \cdot m^2$	Moment of inertia (about z-axis)
d	0.15	m	Length of the quadrotor arm
m	2	kg	Mass
g	9.81	m/s^2	Gravitational acceleration
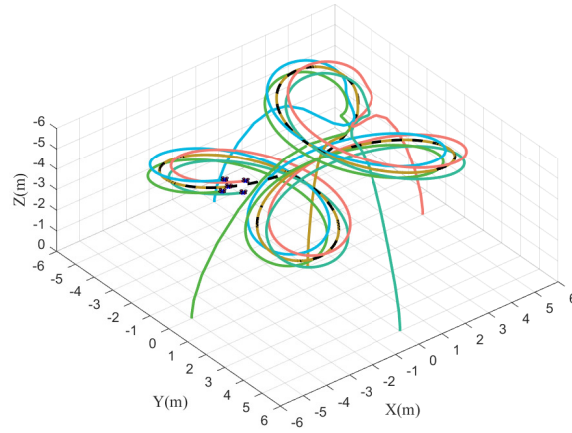
FIGURE 2 Position trajectories of multi-quadrotor systems with EDMPC in 3D space.
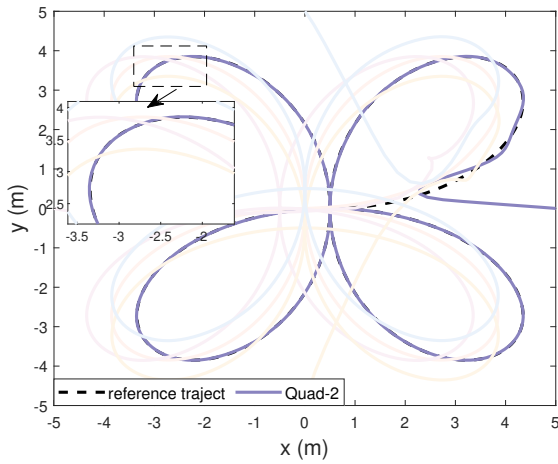
(a)
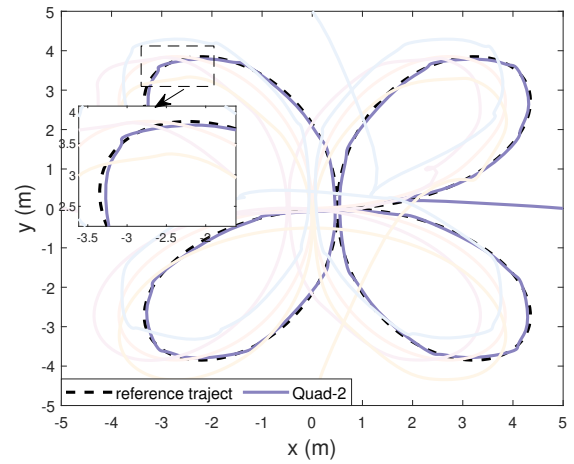
(b)

FIGURE 3 Position trajectory of quadrotor 2 in top view. (a) EDMPC. (b) DMPC.
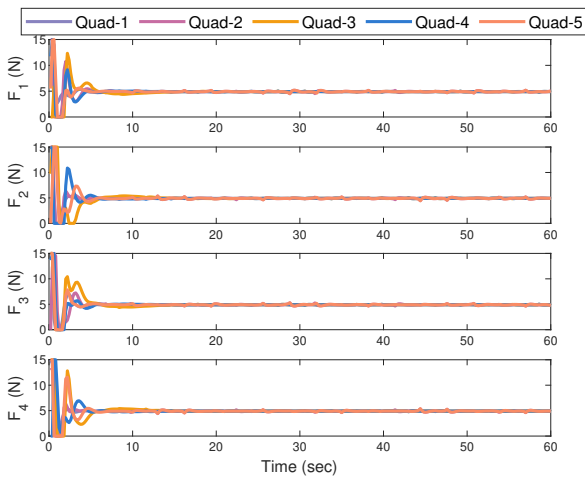
(a)
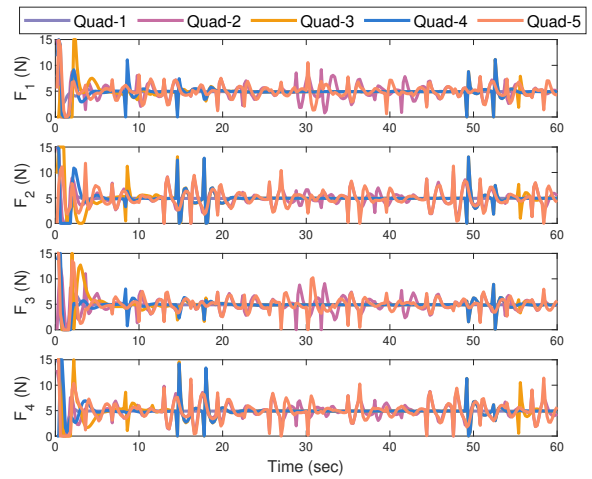
(b)

FIGURE 4 The lift variation curves by each motor of multi-quadrotor systems. (a) EDMPC. (b) DMPC.

TABLE 2 Positions of Multi-quadrotor Systems

Quadrotor	Initial Position (m)	Relative Position to Leader (m)
2	$(5, 0, 0)$	$(0.5, 0, 0)$
3	$(-5, 0, 0)$	$(-0.5, 0, 0)$
4	$(0, -5, 0)$	$(0, -0.5, 0)$
5	$(0, 5, 0)$	$(0, 0.5, 0)$
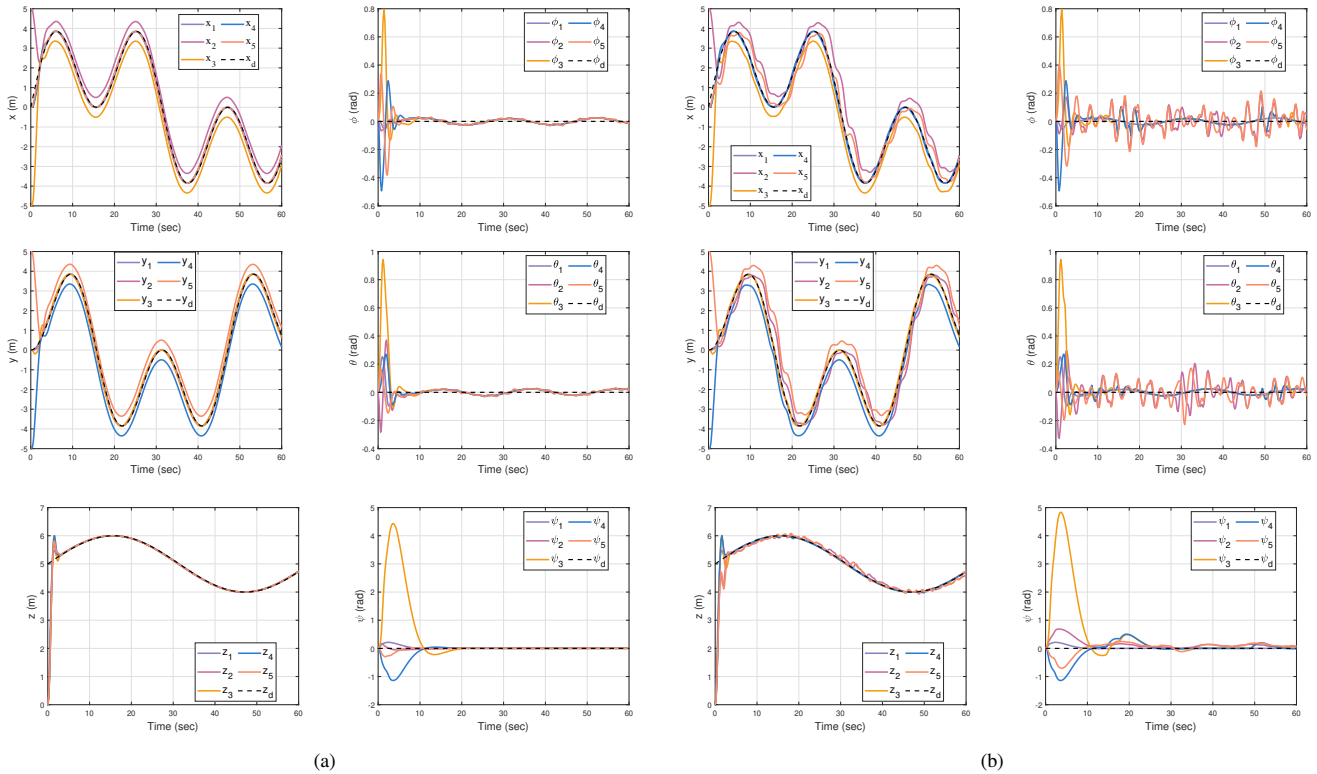
FIGURE 5 Six degrees of freedom states of multi-quadrotor systems. (a) EDMPC. (b) DMPC.

Control input and state constraints are defined as $0 \leq F_{i,n} \leq 15(N)$. Communication delay τ, randomly varying within $[1, \bar{\tau}]$, has an upper limit of $\bar{\tau} = 4$. Other parameters are set as follows: $Q = \text{diag}(100, 1, 100, 1, 100, 1, 1, 1, 1, 1, 1, 1)$, $R = \text{diag}(1, 1, 1, 1)$, $N = 25$, $\Delta t = 0.2$, $\Delta_i = 3.58$, $\zeta = 0.4$, and $\rho_i = \sqrt{6}$. The upper bound of external disturbance is $\bar{\omega} = 0.015$, and the magnitude of disturbance experienced by each quadrotor is generated completely randomly at each time step.

Simulations are conducted using two methods in an environment with time-varying communication delays: the traditional DMPC and the proposed EDMPC. Simulation results, spanning a total of 60 seconds, are presented in Figures 2-6. Figure 2 depicts position trajectories of multi-quadrotor systems in 3D space using EDMPC with communication delays. Figure 3 depicts the position trajectory of the 2nd quadrotor in the top view. Figure 4 shows the lift variation curves by each motor of multi-quadrotor systems, while Figure 5 displays the six degrees of freedom states of multi-quadrotor systems. These results demonstrate the superior performance of quadrotors using the proposed EDMPC approach, particularly considering time-varying communication delay, compared to traditional DMPC.

Figure 6 demonstrates the variation in distances within the formation, indicating that the proposed EDMPC method effectively operates within specified constraints (10). In an environment with time-varying communication delays, the formation distance error is maintained within a reasonable range, [-0.21m, 0.19m], indicating that the multi-quadrotor systems maintain the desired formation more smoothly. Notably, increasing the minimum interval time can significantly alleviate the computational burden,
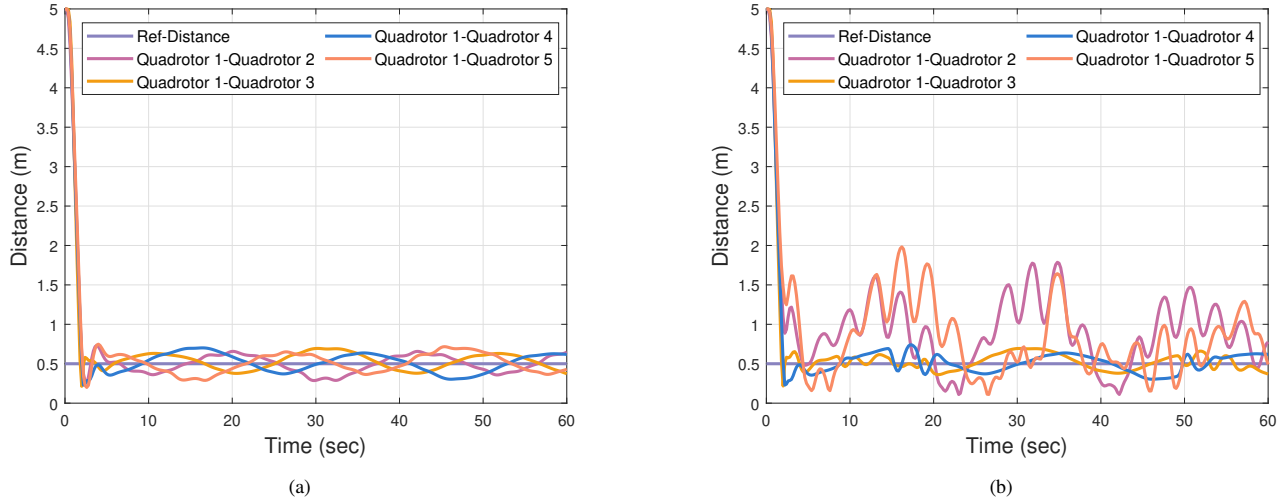
FIGURE 6 The formation distance of multi-quadrotor systems. (a) EDMPC. (b) DMPC.
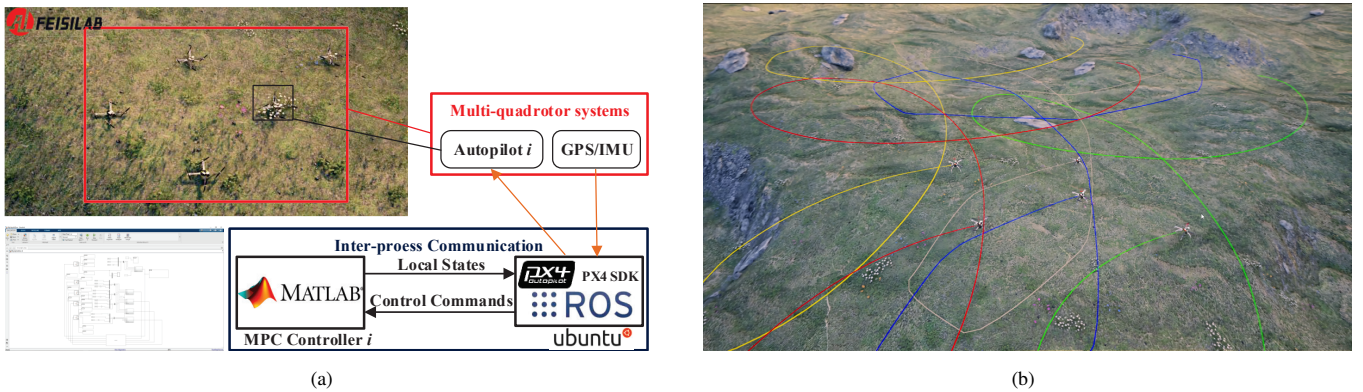
FIGURE 7 (a) EDMPC framework for the SIL simulations. (b) Position trajectories of multi-quadrotor systems with EDMPC in SIL.

albeit at the expense of tracking performance. Therefore, a trade-off is evident between maintaining overall system formation stability and minimizing the communication and computational load.

To further testify the validity of the proposed EDMPC strategy, experiments using the SIL real-time simulations are also conducted. The SIL real-time simulation is implemented using solvers designed by the Simulink Real-Time Toolbox. The quadrotor model runs in the Robot Operating System (ROS) environment, utilizing the RflySim software development kit developed based on PX4 and ROS. Communication between the multi-quadrotor systems is achieved through interprocess communication, with the addition of random communication delays of up to four sampling periods. These measures increase the realism of the simulation. A detailed schematic illustration of the control system in the SIL simulations is shown in Figure 7(a). Figure 7(b) of RflySim3D depicts the monitored trajectories and dynamics of the multi-quadrotor systems throughout the entire mission process. The simulation results indicate that the proposed EDMPC method can cope with complex time-varying communication delays and achieve the task of formation composition and keeping. These results validate the effectiveness and reliability of the proposed EDMPC approach for formation composition and keeping missions of multi-quadrotor systems in time-varying communication delay scenarios.

6 | CONCLUSION

This paper proposes an EDMPC approach to address the formation composition and maintenance problem of multi-quadrotor systems in a complex environment with time-varying communication delays. In the approach, an ETM is employed to reduce bandwidth usage in the multi-quadrotor systems, providing support for stable formation composition and keeping control. To address the issue of time-varying communication delays in multi-quadrotor systems, a novel consistency constraint is introduced to ensure that deviations between the latest predicted state and previously predicted states remain within a predefined region. This strategy ensures that the multi-quadrotor systems maintain a certain level of formation accuracy under any communication delays. Simulation results demonstrate that, compared to traditional DMPC methods in environments with time-varying communication delays, the proposed EDMPC approach significantly reduces communication load and enhances the stability of multi-quadrotor formation control. However, real-world scenarios in multi-quadrotor systems often pose challenges such as packet loss and network attacks, for which effective solutions are still under development. Improving the ability of multi-quadrotor systems to cope with communication packet loss and destructive attacks will be the direction of future research.

References

1. Fei B, Bao W, Zhu X, Liu D, Men T, Xiao Z. Autonomous cooperative search model for multi-UAV with limited communication network. *IEEE Internet of Things Journal* 2022; 9(19): 19346-19361.

2. Liang X, Yu H, Zhang Z, Liu H, Fang Y, Han J. Unmanned aerial transportation system with flexible connection between the quadrotor and the payload: modeling, controller design, and experimental validation. *IEEE Transactions on Industrial Electronics* 2023; 70(2): 1870-1882.

3. Wang R, Wang K, Song W, Fu M. Aerial-Ground collaborative continuous risk mapping for autonomous driving of unmanned ground vehicle in Off-Road Environments. *IEEE Transactions on Aerospace and Electronic Systems* 2023; 59(6): 9026-9041.

4. Schedl DC, Kurmi I, Bimber O. An autonomous drone for search and rescue in forests using airborne optical sectioning. *Science Robotics* 2021; 6(55): eabg1188.

5. Giordan D, Adams MS, Aicardi I, et al. The use of unmanned aerial vehicles (UAVs) for engineering geology applications. *Bulletin of Engineering Geology and the Environment* 2020; 79(7): 3437-3481.

6. Alsuhli G, Fahim A, Gadallah Y. A survey on the role of UAVs in the communication process: A technological perspective. *Computer Communications* 2022; 194: 86-123.

7. Wang Y, Cao J, Kashkynbayev A. Multi-agent bifurcation consensus-based multi-layer UAVs formation keeping control and its visual simulation. *IEEE Transactions on Circuits and Systems I: Regular Papers* 2023; 70(8): 3221-3233.

8. Hua C, Chen J, Guan X. Dynamic surface based tracking control of uncertain quadrotor unmanned aerial vehicles with multiple state variable constraints. *IET Control Theory & Applications* 2019; 13(4): 526-533.

9. Liu H, Ma T, Lewis FL, Wan Y. Robust formation trajectory tracking control for multiple quadrotors with communication delays. *IEEE Transactions on Control Systems Technology* 2020; 28(6): 2633-2640.

10. Pan YJ, Werner H, Huang Z, Bartels M. Distributed cooperative control of leader–follower multi-agent systems under packet dropouts for quadcopters. *Systems Control Letters* 2017; 106: 47-57.

11. Abbasi SH, Mahmood A, Khaliq A, Imran M. LQR controller for stabilization of bio-inspired flapping wing UAV in gust environments. *Journal of Intelligent & Robotic Systems* 2022; 105(4): 79.

12. Huang Q, Zhang E, Dai X, Wu Q, Su S. Sliding-mode fault-tolerant control of the six-rotor UAV with dead-zone-input under event-triggered mechanism. *ISA transactions* 2024; 145: 19-31.

13. Zhang Y, Chen Z, Zhang X, Sun Q, Sun M. A novel control scheme for quadrotor UAV based upon active disturbance rejection control. *Aerospace Science and Technology* 2018; 79: 601-609.

14. Wang Y, Zhang T, Cai Z, Zhao J, Wu K. Multi-UAV coordination control by chaotic grey wolf optimization based distributed MPC with event-triggered strategy. *Chinese Journal of Aeronautics* 2020; 33(11): 2877-2897.

15. Wehbeh J, Rahman S, Sharf I. Distributed model predictive control for UAVs collaborative payload transport. *2020 IEEE/RSJ International Conference on Intelligent Robots and Systems (IROS)* 2020: 11666-11672.

16. Zou Y, Su X, Li S, Niu Y, Li D. Event-triggered distributed predictive control for asynchronous coordination of multi-agent systems. *Automatica* 2019; 99: 92-98.

17. Cui M, Tong S. Event-triggered predefined-time output feedback control for fractional-order nonlinear systems with input saturation. *IEEE Transactions on Fuzzy Systems* 2023; 31(12): 4397-4409.

18. Huang Y, Deng F, Wan F. Event-triggered control for stochastic systems with multiple delays. *International Journal of Robust and Nonlinear Control* 2023; 33(1): 641-658.

19. Yoo J, Johansson KH. Event-triggered model predictive control with a statistical learning. *IEEE Transactions on Systems, Man, and Cybernetics: Systems* 2021; 51(4): 2571-2581.

20. Jang D, Son CY, Yoo J, Kim HJ, Johansson KH. Efficient networked UAV control using event-triggered predictive control. *IFAC-PapersOnLine* 2019; 52(15): 412-417.

21. Li H, Shi Y. Event-triggered robust model predictive control of continuous-time nonlinear systems. *Automatica* 2014; 50(5): 1507-1513.

22. Cano JM, Lopez-Martinez M, Acosta J Network adapter for sampled linear systems under asynchronous and delayed communications: quadrotor remote speed control through cellular network. *IEEE Transactions on Control Systems Technology* 2022; 30(4): 1736-1741.

23. Rochefort Y, Piet-Lahanier H, Bertrand S, Beauvois D, Dumur D. Model predictive control of cooperative vehicles using systematic search approach. *Control Engineering Practice* 2014; 32: 204-217.

24. Zhu W, Cheng D. Leader-following consensus of second-order agents with multiple time-varying delays. *Automatica* 2010; 46(12): 1994-1999.

25. Zhan J, Jiang ZP, Wang Y, Li X. Distributed model predictive consensus with self-triggered mechanism in general linear multiagent systems. *IEEE Transactions on Industrial Informatics* 2019; 15(7): 3987-3997.

26. El-Ferik S, Siddiqui BA, Lewis FL. Distributed nonlinear MPC of multi-agent systems with data compression and random delays. *IEEE Transactions on Automatic Control* 2016; 61(3): 817-822.

27. Wei H, Zhang K, Shi Y. Self-triggered min–max DMPC for asynchronous multiagent systems with communication delays. *IEEE Transactions on Industrial Informatics* 2022; 18(10): 6809-6817.

28. Gu X, Xian B, Wang Y. Agile flight for a quadrotor via robust geometry control: Theory and experimental verification. *International Journal of Robust and Nonlinear Control* 2022; 32(7): 4236-4250.

29. Aspragkathos SN, Sinani M, Karras GC, Panetsos F, Kyriakopoulos KJ. An event-triggered visual servoing predictive control strategy for the surveillance of contour-based areas using multirotor aerial vehicles. *2022 IEEE/RSJ International Conference on Intelligent Robots and Systems (IROS)* 2022; 1(22): 2203-2210.